Liquid Backmixing in Bubble Columns and the Axial Dispersion Coefficient

Sujatha Degaleesan and Milorad P. Duduković
Chemical Reaction Engineering Laboratory, Dept. of Chemical Engineering,
Washington University, St. Louis, MO 63130

Liquid backmixing in bubble columns is commonly described using the 1-D axial dispersion model, wherein all the contributing mechanisms leading to liquid macromixing are lumped into a single axial dispersion coefficient. No relationship has been reported that allows the quantification of various fluid-dynamic contributions to the axial dispersion coefficient in bubble columns. In this study, a Taylor-type analysis was performed to arrive at an expression for the axial dispersion coefficient in terms of the two dominant fluid-dynamic factors, convective recirculation and eddy diffusion. Experimental measurements of the relevant fluid-dynamic parameters are used to study the effects of operating conditions on the axial dispersion coefficient and its contributing factors.

Introduction

Bubble-column reactors are widely used in the chemical, petrochemical, biochemical and metallurgical industries. Their lack of moving parts and excellent heat- and mass-transfer characteristics are some of the prominent advantages that render them particularly attractive for various multiphase exothermic reactions. Bubble columns are often designed with a length-to-diameter ratio, or aspect ratio, of at least 5. They are operated in either semibatch mode (zero liquid throughput), such as in liquid-phase methanol synthesis, or continuous mode (cocurrent or countercurrent) such as in Fischer–Tropsch synthesis, with liquid superficial velocities lower than the gas superficial velocity by at least an order of magnitude. As a result, it is the gas flow that controls the fluid dynamics of the individual phases in these systems. This in turn controls liquid mixing and interphase mass transfer, which subsequently influence conversion and selectivity.

In the most basic model for the design of bubble-column reactors one assumes ideal mixing patterns for the gas and liquid phases (e.g., complete backmixing for the liquid and plug flow for the gas phase). Such ideal flow patterns do not exist in these reactors, however, and such an assumption may cause design calculations to deviate from reality. It has been shown, even for simple kinetics, that the assumption of complete mixing of the liquid phase results in considerable oversizing of the reactor, especially for close to complete conversions (Myers et al., 1987). To account for the nonideality in the flow pattern, the one-dimensional (1-D) axial dispersion model (ADM) is most frequently used in bubble-column reactor modeling.

It is by now well understood that liquid mixing in bubble columns is a result of various contributing mechanisms. These include global convective recirculation of the liquid phase, which is induced by the nonuniform gas radial holdup distribution (Devanathan et al., 1990), turbulent diffusion due to the eddies generated by the rising bubbles (Fan and Tsuchiya, 1990), and molecular diffusion, which compared to the other factors is negligible. Turbulent diffusion arises from motion on many scales and reflects both large-scale fluctuations caused by the large-scale eddies, and small-scale fluctuations arising from the entrainment of liquid in the wakes of the fast-rising bubbles.

As was just mentioned, the most common approach to modeling liquid mixing in bubble columns is by using the 1-D axial dispersion model. In this model, all the previously mentioned mechanisms leading to liquid macromixing are lumped into a single axial dispersion coefficient. The immense popularity of the model is due to its simplicity and ease of use, although its ability to describe two-phase flows with large de-

Correspondence concerning this article should be addressed to S. Degaleesan.
Present address of S. Degaleesan: Shell Oil Company, Houston, TX.

grees of backmixing, such as those in bubble columns, is somewhat questionable (Wen and Fan, 1975; Levenspiel and Fitzgerald, 1983). Despite this lack of a sound basis for its application to bubble columns, the ADM still remains extremely popular and numerous correlations for the liquid axial dispersion coefficient in bubble columns have been developed over the years.

The majority of these correlations (summarized by Fan, 1989) are purely empirical in nature. However, there have been attempts made to derive a theoretical or semitheoretical relation for the axial dispersion coefficient based on various assumptions. The concepts involved in various analyses presented in the literature are briefly reviewed here. Baird and Rice (1975) assumed the validity of Kolmogorov's theory of isotropic turbulence, and by dimensional analysis established that the axial dispersion coefficient can be expressed by

$$D_{\text{ax}} = K_r l_e^{4/3} P_m^{1/3}, \tag{1}$$

where l_e is the characteristic length scale of the eddies that are primarily responsible for eddy diffusion, and P_m is the specific energy dissipation rate per unit mass that can be expressed as $P_m = U_g g$ for bubble columns. Assuming that the size of the characteristic eddy is of the order of the column diameter, D_c, Baird and Rice (1975) obtained

$$D_{\text{ax}} = K_r D_c^{4/3} (U_g g)^{1/3}. \tag{2}$$

The constant K_r was taken to be 0.35 based on fitting of experimental data for the dispersion coefficient over a wide range of operating conditions. This correlation is among the most widely used for estimating the extent of liquid backmixing in bubble columns. Its popularity is due to the clear physical basis of the correlation and the fact that the axial dispersion coefficient can be estimated from a known design (e.g., D_c) and operating conditions (e.g., U_g).

Several researchers have attempted to evaluate the axial dispersion coefficient from the multiple circulation cells model by correlating it in terms of the mean circulation velocity. By postulating the existence of axially symmetric steady multiple circulation cells in the column and using the energy balance, Joshi and Sharma (1979) derived an expression for the average liquid circulation velocity. They correlated the liquid-phase axial dispersion coefficient with the liquid recirculation velocity as

$$D_{\text{ax}} = 0.31\, D_c^{1.5} u_{Lc}; \quad u_{Lc} = 1.4[D_c g(U_g - \epsilon_g u_{b\infty})]^{1/3} \tag{3}$$

indicating that the dispersion coefficient is directly proportional to the liquid recirculating velocity. The agreement of their correlation with experimental data is quite good for small-diameter columns. However, the existence of multiple cells in the time-averaged sense, on which this model is based, has not been experimentally verified, which makes the physical basis of the model questionable. The instantaneous flow pattern does exhibit the presence of eddies and vortical structures (Chen et al., 1994). These structures are highly transient and get averaged out, resulting in global liquid recirculation in the time-averaged sense, which does not exhibit multiple cells (Devanathan et al., 1990).

Groen et al. (1995) attempted to develop a physical basis for the axial dispersion coefficient using the concept of the "swarm velocity." They utilized a glass-fiber (optical) probe to measure the local gas holdup in the column. In addition, by simultaneously using probes positioned at two axial positions, they applied cross-correlation techniques to study the dynamics of the flow. At low gas flow rates they estimated the lifetime of an eddy to be about 0.5 s, and the length scale in the axial direction to be the size of the column diameter. They showed that at low gas velocities the flow can be characterized by a single dominant swarm velocity. It appears that, based on the radial position of measurement, the probes were capturing the maximum upward and downward velocities. The axial dispersion coefficient was modeled as

$$D_{\text{ax}} = K_g u D_c, \tag{4}$$

where u is the swarm velocity, which for low superficial gas velocities is claimed to be a constant value within the column. The constant K_g was assumed to be unity. The results of the preceding model were shown to compare well with experimental data for D_{ax} at low superficial gas velocities in the homogeneous bubbly flow regime. The model is appealing since it is based on experimental measurements of the fluid-flow parameters. The database is not broad enough, however, to assess the effect of operating conditions (gas velocity, physical properties, pressure, etc.) on the swarm velocity. At higher gas flow rates in the churn-turbulent flow regime it is expected that several scales and frequencies will be dominant, so that the preceding approach is questionable.

In contrast to the previously expressed theories, which relate the axial dispersion coefficient to the liquid velocity in circulation cells and the bubble swarm velocity, Riquarts (1981) attributes the axial dispersion coefficient only to stochastic mixing caused by the motion of the rising bubbles, and not from circulation. In his analysis, Riquarts starts with a mass balance for a steady-state experiment, by considering liquid upflow in the core and downflow in the annular portion of the column. He assumes, however, that the tracer concentrations in the core region and annular regions are identical and neglects radial diffusion, leading to an oversimplification of the model equations. As a result, the axial dispersion coefficient appearing in the 1-D axial dispersion model has contributions only from stochastic mixing (i.e., axial eddy diffusion). This is physically counterintuitive, since it is established that the large degrees of liquid backmixing in bubble columns are a result of liquid recirculation. The expression for the axial dispersion coefficient obtained by Riquarts is

$$Bo = 14.7\left(\frac{Fr^3}{Re}\right)^{0.125} \tag{5}$$

where $Bo = U_g D_c / D_{\text{ax}}$, $Fr = U_g^2/(D_c g)$, and $Re = U_g D_c / \nu_l$. The constant 14.7 was obtained by fitting the expression to experimental data.

Most of the existing correlations for the axial dispersion coefficient are developed and fitted to data for air–water systems at atmospheric conditions. As a result, these correlations severely underpredict the axial dispersion coefficient in industrial bubble-column reactors that operate under high-pressure conditions, and cannot be applied to such conditions. In addition, a majority of industrial systems have internal heat-exchanger tubes, which have also been shown to increase the axial dispersion coefficient (Berg et al., 1995). To account for the effects of the heat-exchanger tubes Berg et al. (1995) proposed the following correlation

$$D_{ax} = 0.208 U_g^{0.4} (D_c + N_R d_R)^{1.48} \phi_s^{1.8} \nu_l^{-0.12} \quad \text{SI units,} \quad (6)$$

where N_R is the total number of tubes, d_R is the outer diameter of the tubes, ϕ_s is the relative free area, and ν_l is the kinematic viscosity of the liquid. The empirical constant, 0.208, was obtained by fitting experimental data from heat tracer experiments. It is noted that the dispersion coefficients obtained from these experiments are consistently higher than the results obtained using traditional backmixing experiments, such as conductivity and spectrophotometric methods.

Wilkinson et al. (1993) formulated a mechanistic model to account for liquid mixing in bubble columns caused by convection along with axial dispersion and radial turbulent exchange. The objective was to study the effect of pressure on liquid backmixing. By making several simplifying assumptions in their model, they arrived at an expression for the axial dispersion coefficient in terms of the convective liquid velocity, $\bar{u}_l$; axial eddy dispersion coefficient, E; and a radial exchange term, K, as given by the following equation:

$$D_{ax} = E + \frac{\bar{u}_l D_c \sqrt{2}}{16(1-\epsilon_g)^2 K}. \quad (7)$$

However, due to the unknown values of the eddy dispersion coefficient and exchange factor (which are functions of operating conditions), quantitative estimates of the dispersion coefficient using this expression could not be made. They experimentally measured the liquid-phase dispersion coefficient in air–water systems at high pressure, and showed that there is an increase in D_{ax} with pressure. The existing literature correlations were shown to underpredict the axial dispersion coefficient under high-pressure conditions.

Several attempts have also been made in performing a Taylor-type analysis to arrive at an expression for the axial dispersion coefficient. Mashelkar and Ramachandran (1975) derived an expression by assuming negligible axial eddy diffusivity, for viscous chain bubbling. The flow regime in which their expression is applicable is not of interest in the present investigation. Ohki and Inoue (1970) developed a dispersion model in the bubbly flow regime, by essentially modifying the Taylor–Aris approach. Assuming a uniform turbulent diffusivity in the column, they arrived at the following expression for the dispersion coefficient:

$$D_{ax} = 0.30 D_c^2 U_g^{1.2}, \quad (8)$$

In the churn-turbulent flow regime the model parameters could not be directly evaluated from first principles.

Miyauchi et al. (1981) considered the effects of the radial recirculating velocity profile (Ueyama and Miyauchi, 1979), along with radial and axial turbulent diffusion, in estimating the axial dispersion coefficient. Their final expression for the dispersion coefficient is given by

$$D_{ax} = 0.5 g^{1/4} U_g^{1/2} D_c^{5/4}. \quad (9)$$

The drawback of their analysis was that a constant gas holdup was assumed throughout the cross section of the column. This was shown by Myers (1986) to lead to inconsistencies in the equations describing the flow. In addition to this, since measurements for the turbulent diffusivities were not available, the radial diffusivity was assumed to be equal to the eddy viscosity associated with the one-equation closure model for the turbulent shear stress used in the momentum balance equation (Ueyama and Miyauchi, 1979). The axial turbulent diffusivity had to be fitted to match experimental results for the axial dispersion coefficient. Anderson (1989), in a similar type of analysis, assumed an average gas holdup instead of a profile in addition to neglecting the axial eddy diffusivity, and therefore was not able to achieve good comparison with experimental dispersion coefficients. It is shown later in this article that the axial eddy diffusivity makes a considerable contribution to the liquid axial dispersion coefficient.

Despite the various attempts at using a theoretical or semitheoretical approach in obtaining an expression for the axial dispersion coefficient, there still exists no relationship that quantifies the contributions of the different mechanisms to overall liquid backmixing in bubble columns, described by the axial dispersion coefficient. In the present work such a quantification has been accomplished, by adopting a Taylor-type analysis and using experimental data from Computer Automated Radioactive Particle Tracking (CARPT) measurements for the various fluid dynamic quantities. Our objective was to relate the axial dispersion coefficient to the key fluid dynamic parameters, determine these parameters experimentally, and establish the effect of operating conditions on such parameters and the axial dispersion coefficient.

Contributions of Convection and Eddy Diffusion to Liquid Backmixing in Bubble Columns

In this section a Taylor-type analysis of the fundamental 2-D axisymmetric convection–diffusion equation for liquid mixing in bubble columns is performed, to arrive at an expression for the effective axial dispersion coefficient in terms of the two dominant factors contributing to liquid backmixing: convective recirculation and (axial and radial) eddy diffusion.

The analysis is restricted to systems with low superficial liquid velocities, wherein the cross-sectional average liquid velocity relative to local liquid velocities is negligible. A steady backmixing experiment is considered, as depicted in Figure 1, in a bubble column of large aspect ratio (typically $L/D > 5$), with cocurrent gas and liquid flow. Under such conditions, with sufficient gas flow rate, most of the column is occupied by a single liquid recirculation cell, in the time-averaged sense (Devanathan et al., 1990). A continuous stream of liquid tracer is introduced uniformly at the top of the column. The liquid flow rate through the column can be as low as possible, just sufficient enough to ensure an outflow of liquid that can carry the tracer. The governing equation for the liquid-confined tracer, in the presence of assumed angular symmetry, is a 2-D convection-diffusion equation:

$$\frac{1}{r}\frac{\partial}{\partial r}\epsilon(r)D_{rr}(r)r\frac{\partial C}{\partial r}=\epsilon(r)u_z(r)\frac{\partial C}{\partial z}-\epsilon(r)D_{zz}(r)\frac{\partial^2 C}{\partial z^2}. \tag{10}$$

The preceding equation is written for the well-developed flow region in the column (middle portion of the recirculation cell), where experimental evidence indicates that the time-averaged liquid holdup, ϵ; axial liquid velocity, u_z; eddy diffusivities in the radial, D_{rr}; and axial directions, D_{zz}, are functions of radial position only, radial velocities are zero, and end effects can be neglected (Degaleesan, 1997). Our objective is to show that Eq. 10 can be replaced by the well-known axial dispersion model for the cross-sectional mean liquid tracer concentration, $\overline{C}$, given by

$$D_{\text{eff}}\frac{d^2\overline{C}}{dz^2}-\overline{u}\frac{d\overline{C}}{dz}=0 \tag{11}$$

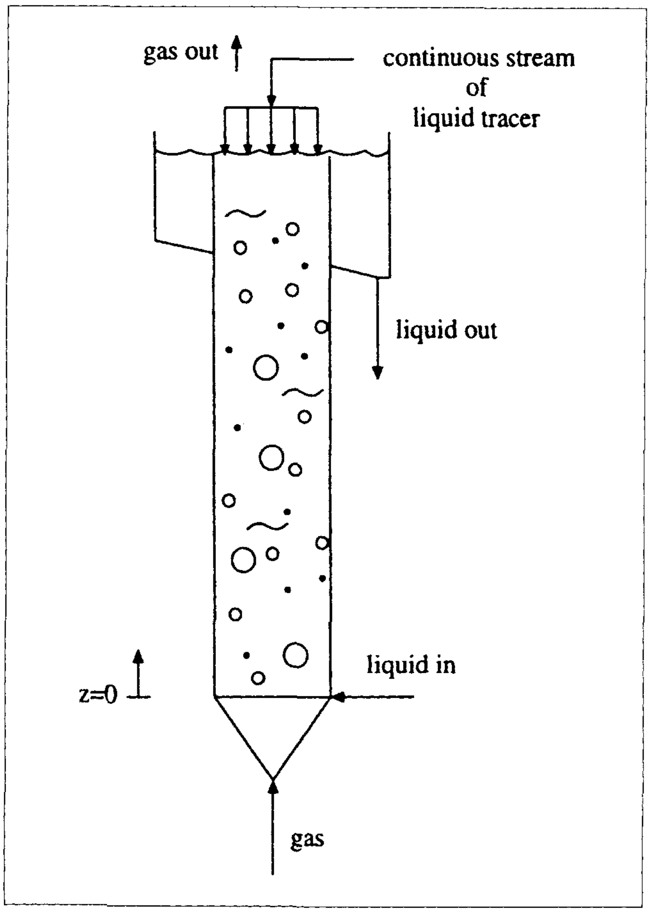

Figure 1. Steady backmixing experiment.

where $\overline{u}$ $(=U_l/\epsilon)$ is the cross-sectional average liquid interstitial velocity, and to establish the relationship between the axial dispersion coefficient, D_{eff}, and the fundamental fluid dynamic parameters contained in Eq. 10.

Simulation results of Eq. 10 (a sample is shown in Figure 2), using experimental measurements for the fluid-dynamic parameters ϵ, u_z, D_{rr}, and D_{zz}, allows us to decompose the liquid tracer concentration $C(r,z)$ into two parts:

$$C(r,z)\equiv\overline{C}(z)+C'(r,z), \tag{12}$$

where $\overline{C}$ is the cross-sectional average concentration, which is a function of axial position only, and C' represents the radial variation of the local concentration about the mean concentration and has a cross-sectional mean of zero; C' is a function of both radial and axial position. In addition, simulation results indicate that C' is only a mild function of z. In other words,

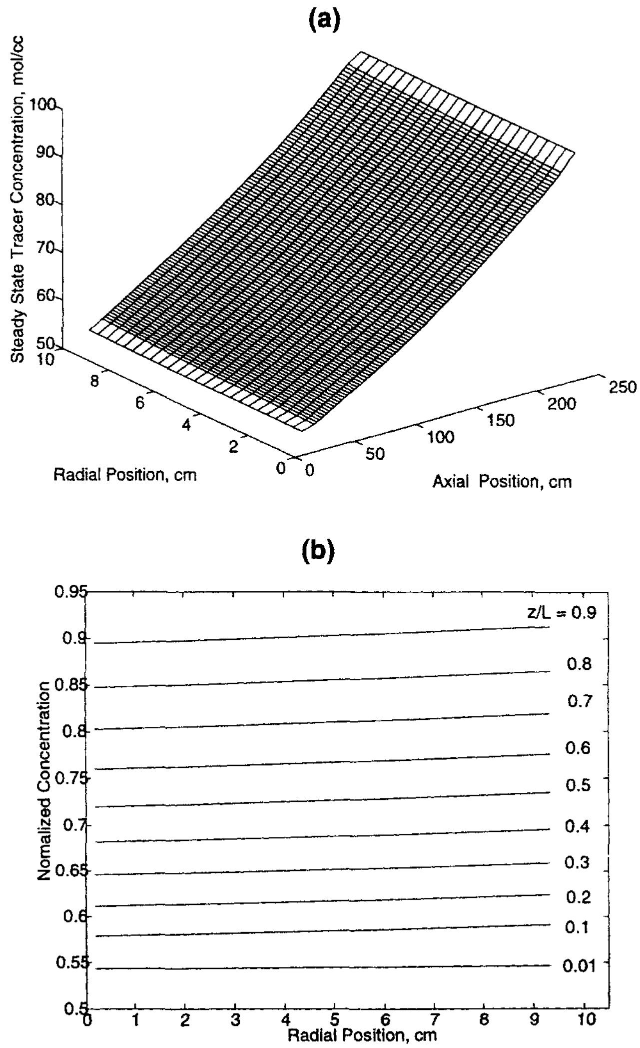

Figure 2. Simulation results (maximum concentration normalized) of the steady-state 2-D convection diffusion model for $D_c = 19$ cm, $U_g = 10$ cm/s, $U_l = 1$ cm/s.

$$\frac{\partial C'}{\partial z} \ll \frac{d\overline{C}}{dz} \quad \text{and} \quad \frac{\partial^2 C'}{\partial z^2} \ll \frac{d^2\overline{C}}{dz^2}. \tag{13}$$

For example, considering the case shown in Figure 2, a typical value for $d\overline{C}/dz = 0.397$ (arb. units) and $\partial C'/\partial z = 0.003$ (arb. units). Hence it can be assumed that

$$\frac{\partial C'}{\partial z} \sim 0 \quad \text{and} \quad \frac{\partial^2 C'}{\partial z^2} \sim 0 \tag{14}$$

Using the preceding assumptions and substituting Eq. 12 into Eq. 10 gives:

$$\frac{1}{r}\frac{d}{dr}\epsilon(r)D_{rr}(r)r\frac{dC'(r,z)}{dr} = \epsilon(r)u_z(r)\frac{d\overline{C}(z)}{dz} - \epsilon(r)D_{zz}(r)\frac{d^2\overline{C}(z)}{dz^2}. \tag{15}$$

Experimental evidence from the literature (Argo and Cova, 1965; Ohki and Inoue, 1970; Myers, 1986) and simulation results of Eq. 10 (see Figure 2) indicate that the cross-sectional mean concentration, $\overline{C}$, is an (mild) exponential function of axial position, $\exp(k_z z)$, which automatically satisfies Eq. 11 ($k_z = \overline{u}/D_{\text{eff}}$). Hence,

$$\overline{C}(z) = C_0 \exp(k_z z), \tag{16}$$

where C_0 is an arbitrary constant, satisfies Eq. 17,

$$\frac{\partial^2 \overline{C}}{\partial z^2} = k_z \frac{\partial \overline{C}}{\partial z}. \tag{17}$$

By substituting the preceding result into Eq. 15, we get

$$\frac{1}{r}\frac{d}{dr}\epsilon(r)D_{rr}(r)r\frac{dC'(r,z)}{dr} = \frac{d\overline{C}(z)}{dz}\left[\epsilon(r)u_z(r) - \epsilon(r)D_{zz}(r)k_z\right]. \tag{18}$$

The following is obtained after double integration over r, with symmetry conditions at the center and zero flux at the wall:

$$C'(z,r) = \frac{d\overline{C}(z)}{dz} I2(r) + C'(0,z), \tag{19}$$

where

$$I2(r) = \int_0^r \frac{I(r')}{r'\epsilon(r')D_{rr}(r')} dr' \tag{20}$$

$$I(r) = \int_0^r r'\epsilon(r')[u_z(r') - D_{zz}(r')k_z]\, dr' \tag{21}$$

and

$$C'(0,z) = -\frac{d\overline{C}(z)}{dz} \frac{\int_0^R I2(r) r\epsilon(r)\, dr}{\int_0^R r\epsilon(r)\, dr}. \tag{22}$$

An average tracer flux for a cross section of the column can now be defined as

$$J = \underbrace{\frac{\int_0^R r\epsilon(r)u_z(r)C(r,z)\, dr}{\int_0^R r\epsilon(r)\, dr}}_{T1} - \underbrace{\frac{\int_0^R \epsilon(r) r D_{zz}(r)\, dr}{\int_0^R r\epsilon(r)\, dr}\frac{\partial \overline{C}}{\partial z}}_{T2}. \tag{23}$$

Substituting Eq. 12 for $C(r,z)$ in the first term of Eq. 23, the integral involving $\overline{C}$ can be dropped, as it is close to zero (due to the low liquid superficial velocities considered), giving the following expression for $T1$:

$$T1 = \frac{\partial \overline{C}(z)}{\partial z}\left(\frac{\int_0^R r\epsilon(r)u_z(r) I2(r)\, dr}{\int_0^R r\epsilon(r)\, dr}\right) = -\frac{d\overline{C}(z)}{dz} D_{\text{Taylor}}, \tag{24}$$

where D_{Taylor} is the Taylor-type diffusivity that arises due to convective mixing, and is given by Eq. 29. The second term in Eq. 23 can be written as

$$T2 = \overline{D}_{zz}\frac{d\overline{C}(z)}{dz}. \tag{25}$$

Substituting for $T1$ and $T2$ in Eq. 23 gives

$$J = -\frac{\partial \overline{C}(z)}{\partial z}\left[D_{\text{Taylor}} + \overline{D}_{zz}\right] = -\frac{\partial \overline{C}(z)}{\partial z} D_{\text{eff}}. \tag{26}$$

The effective axial dispersion coefficient is therefore

$$D_{\text{eff}} = D_{\text{Taylor}} + \overline{D}_{zz}. \tag{27}$$

Clearly, both Taylor-type diffusivity and the mean axial eddy diffusivity contribute to the axial dispersion coefficient. The mean axial eddy diffusivity is nothing but the cross-sectional average of the axial eddy diffusivity, that is,

$$\overline{D}_{zz} = \frac{\int_0^R \epsilon(r) r D_{zz}(r)\, dr}{\int_0^R r\epsilon(r)\, dr}, \tag{28}$$

as is evident from Eq. 23. A review of the preceding analysis and inspection of Eq. 24 reveals that the Taylor diffusivity is given by

$$D_{\text{Taylor}} = \frac{\int_0^R r\epsilon(r)u_z(r)\left(\int_0^r \frac{\int_0^{r'} \tilde{r}\epsilon(\tilde{r})\left[u_z(\tilde{r}) - D_{zz}(\tilde{r})\frac{\bar{u}}{D_{\text{eff}}}\right]d\tilde{r}}{r'\epsilon(r')D_{rr}(r')}dr'\right)dr}{\int_0^R r\epsilon(r)\,dr}. \tag{29}$$

It seems as though a cumbersome trial-and-error problem is at hand since the integrals in Eq. 29 contain D_{Taylor} via the D_{eff} term. However, the analysis of available experimental data reveals that $D_{zz} < D_{\text{eff}}$ and $u_z \gg \bar{u}$ except for the liquid velocity at the velocity inversion point. Hence, the $D_{zz}(\bar{u}/D_{\text{eff}})$ term in Eq. 29 can be neglected. This is true for the often used case of batch liquid when $\bar{u} = 0$ and is a good approximation for low to reasonable liquid superficial velocities of the order of up to 1 cm/s. In such situations D_{Taylor} is a function only of the axial liquid velocity profile, $u_z(r)$, radial liquid holdup profile, $\epsilon(r)$, and radial eddy diffusivity profile, $D_{rr}(r)$.

It is now possible to estimate the contributions of convection (Taylor dispersion) and eddy diffusion to the 1-D axial dispersion coefficient, by evaluating the expressions for D_{Taylor} and $\overline{D}_{zz}$. The 1-D liquid recirculation model (Kumar et al., 1994) that we use for evaluation of the radial profile of the axial liquid velocity (along with experimental measurements for the local liquid holdup and axial liquid velocity) does not permit an analytical solution for the liquid velocity profile. Hence, the evaluation of the previous terms is done by numerically integrating the expressions in Eq. 23.

Our objective to relate the liquid axial dispersion coefficient in bubble columns to the key fluid dynamic parameters has been accomplished in establishing Eqs. 27, 28 and 29. At present, however, the quantities needed for computation of the axial dispersion coefficient, such as the radial liquid holdup profile, radial profile of axial liquid velocity, and radial profiles for the axial and radial eddy diffusivities cannot be predicted from first principles, nor are suitable correlations available. Hence, we resort to obtaining D_{eff} by experimentally measuring all the needed fluid dynamic quantities, in the hope that such a database will reveal a possible way of correlating D_{Taylor} and $\overline{D}_{zz}$ with observable operating parameters.

Experimental Studies

The fluid dynamic parameters required for the evaluation of the axial dispersion coefficient are obtained from experimental measurements. The liquid phase time averaged velocities and eddy diffusivities are measured using the noninvasive CARPT technique (Devanathan, 1991) and liquid-phase holdup distribution using computed tomography (CT) (Kumar, 1994). The experiments were conducted in the Chemical Reaction Engineering Laboratory (CREL) at Washington University.

In the CARPT technique (Yang et al., 1992; Duduković et al., 1997) a single neutrally buoyant tracer particle, 2.36 mm in diameter, that consists of a polypropylene sphere enclosing a radioactive scandium-46 particle and air, is used to track the liquid phase. As the particle moves around the column

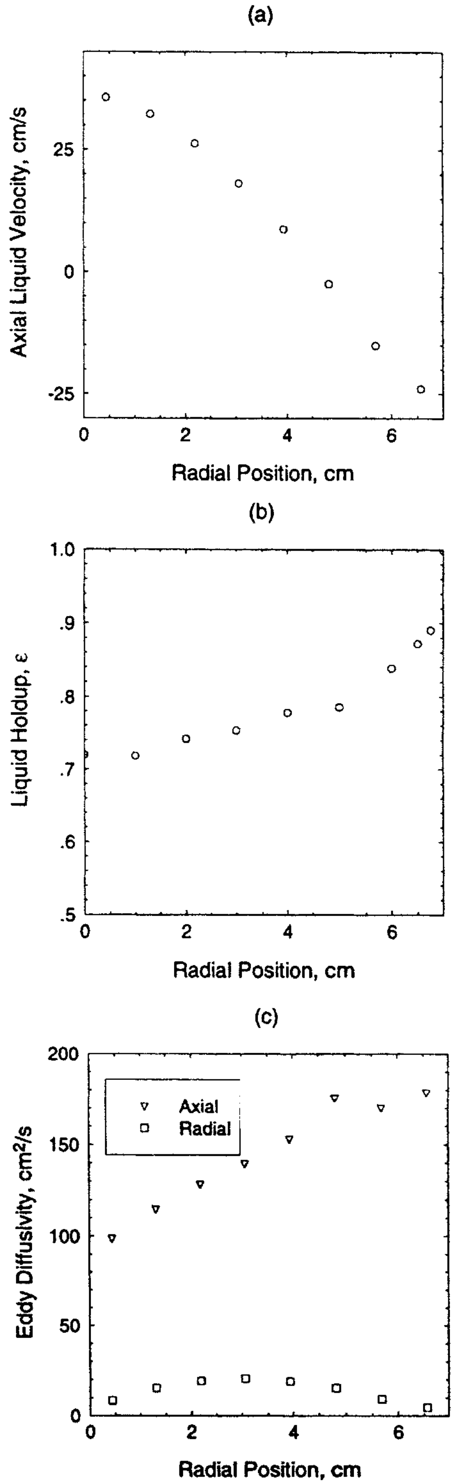

Figure 3. Fluid dynamic parameters in a 14-cm-dia. column (6A), $U_g = 9.6$ cm/s.

(a) Axial liquid velocity profile; (b) liquid holdup profile; (c) axial and radial eddy diffusivities.

tracing the liquid, the γ radiation emitted by the particle is registered by an array of scintillation detectors positioned around the column. After a series of hardware processing steps, this information is stored on the hard drive of a computer as radiation intensity counts per sampling time. The radiation intensity measured by the detectors at a given sampling instant is used to estimate the position of the particle based on a weighted linear regression scheme. Time differencing of particle positions at subsequent time steps yields the instantaneous Lagrangian velocities of the particle, which upon averaging yields the ensemble averaged (time-averaged) velocities and thereafter the turbulence parameters. One of the advantages of CARPT is the ability to measure the eddy diffusivities using the Lagrangian velocities. Additional details regarding the data-processing steps can be found in Degaleesan (1997).

In CT (Kumar, 1994) a hard radioactive source (cesium-137), which emits gamma radiation, is placed in a lead-shielded enclosure. The gamma radiation emitted by the source passes through a slit in the lead enclosure and is used to scan the cross section of the column in operation at several angles. The transmitted radiation, which is measured by a fan-beam array of detectors in the form of attenuation coefficients, is used to reconstruct the time-averaged phase distribution at a given cross-sectional plane. In the present work the data for the void fraction is taken from Kumar (1994) and Chen et al. (1997).

Results and Discussion

CARPT experiments were conducted in air–water systems, in columns of three internal diameters, 14 cm, 19 cm, and 44 cm, and with gas velocities ranging from 2 cm/s to 12 cm/s. Perforated plate distributors made of aluminum were used in all the columns. In the 14-cm column two distributors were used: **6A**, with an open area of 0.05%, and **6B**, with an open area of 0.62%. In general, the turbulence parameters in **6B** are higher than those in **6A** due to the larger hole size and porosity in **6B** (Degaleesan, 1997). Typical results for the radial profiles of the time-averaged liquid velocity, liquid holdup, and axial and radial eddy diffusivities are shown in Figure 3. As Figure 3a indicates, the liquid flows upward in the center of the column and downward near the wall, establishing a recirculation cell over the entire length of the column, in the time-averaged sense. Figure 3c shows typical profiles for axial and radial eddy diffusivities. For a given experimental condition, the axial eddy diffusivity is much larger than the radial eddy diffusivity, by almost an order of magnitude. A more detailed presentation and analysis of the results for the liquid velocities and turbulence parameters are available in Degaleesan (1997).

Figures 4a, 4b and 5 show the effect of operating conditions on $\overline{D}_{zz}$, calculated from Eq. 28; $\overline{D}_{rr}$, defined analogously to Eq. 28; and D_{Taylor}, calculated using Eq. 29. Based on our experimental database, the following simpler functional form is obtained for D_{Taylor}:

$$D_{\text{Taylor}} = \frac{1}{K_T} \frac{\bar{u}_{\text{rec}}^2 R^2}{\overline{D}_{rr}}, \tag{30}$$

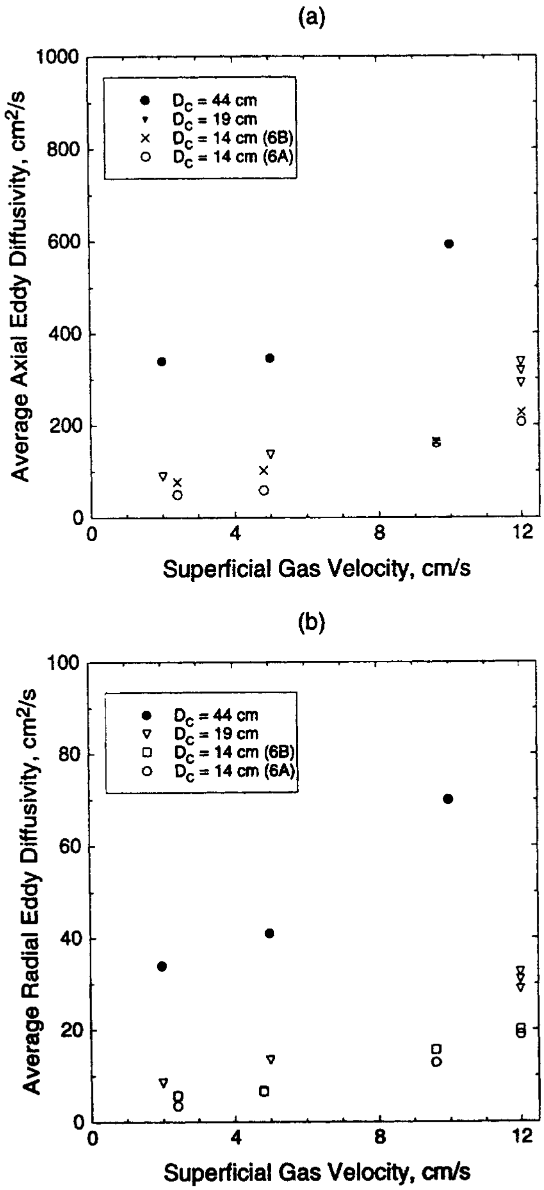

Figure 4. Effect of superficial gas velocity on (a) average axial eddy diffusivity, $\overline{D}_{zz}$; (b) average radial eddy diffusivity, $\overline{D}_{rr}$.

where $\bar{u}_{\text{rec}}$ is the mean liquid recirculating velocity, defined by

$$\bar{u}_{\text{rec}} = \frac{\int_0^{r^*} u_z(r)\epsilon(r) r dr}{\int_0^{r^*} \epsilon(r) r dr} \tag{31}$$

where r^* is the inversion point of the axial liquid velocity profile, and K_T is a (fitted) constant

$$K_T = 14.2 \pm 5.4 \qquad \left(\overline{K}_T \pm 2\sigma_{K_T}\right). \tag{32}$$

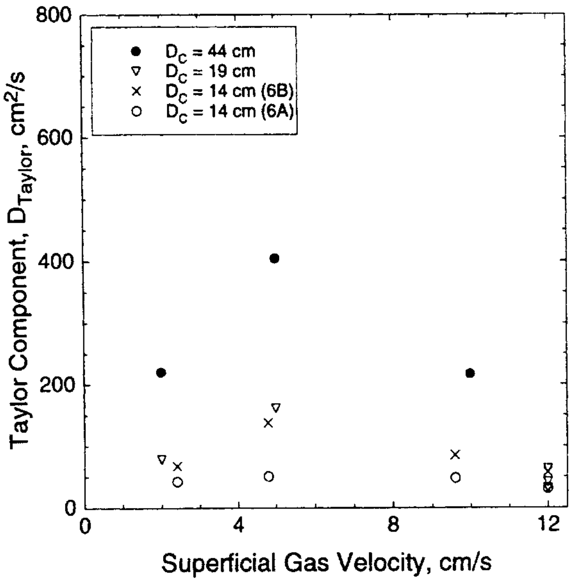

Figure 5. Effect of superficial gas velocity on Taylor component, D_{Taylor}.

The preceding expression for D_{Taylor} is analogous to the celebrated Taylor diffusivity (Taylor, 1954). Since the magnitude of the radial eddy diffusivity is large, the Taylor dispersion term in Eq. 30 contributes only in part to the overall axial dispersion. The axial eddy diffusivity, as seen in Figure 4a, also plays a major role in axial liquid mixing, contrary to the assumption of many researchers in their analyses.

While there is a monotonic increase in $\overline{D}_{zz}$ (Figure 4a) with superficial gas velocity, D_{Taylor} initially increases with gas velocity up to a certain point, beyond which it starts to drop (Figure 5). It appears from the data points that this occurs around the transition regime, which occurs for air–water systems at a gas velocity of about 5 cm/s. This trend reflects the behavior of the liquid recirculation velocity ($\overline{u}_{rec}$) and the eddy diffusivities with gas velocity. At very low gas velocities, convection dominates and the turbulence level is low (Degaleesan, 1997). Hence, there is initially a strong increase in D_{Taylor} (Eq. 30) with gas velocity, in the bubbly flow regime. Then, as the gas velocity is increased into the churn-turbulent flow regime, the increase in eddy diffusivities starts to become more pronounced (transition from bubbly flow to churn-turbulent flow). This increase in $\overline{D}_{rr}$, relative to $\overline{u}_{rec}$, causes D_{Taylor} to decrease. Figure 6 shows the variation of the effective liquid axial dispersion coefficient (obtained from CARPT measurements based on the present analysis) with gas velocity in a 14-cm- and 44-cm-diameter column. At the lower gas velocities, in the bubbly flow regime, the contribution of D_{Taylor} to the axial dispersion coefficient is higher than that of $\overline{D}_{zz}$. With increase in gas velocity the Taylor component decreases. Figure 6 shows the trends up to gas velocities of 12 cm/s, for which CARPT data are currently available. It is expected that with further increase in gas velocity, well into the churn-turbulent regime, the Taylor component will increase again with gas velocity. This expectation is based on the observed trends of the liquid recirculating velocity and the radial eddy diffusivity with gas velocity in the churn-turbulent flow regime, which suggest that the increase of $\overline{u}_{rec}$ with gas velocity is relatively larger than that of $\overline{D}_{rr}$ (Degaleesan, 1997).

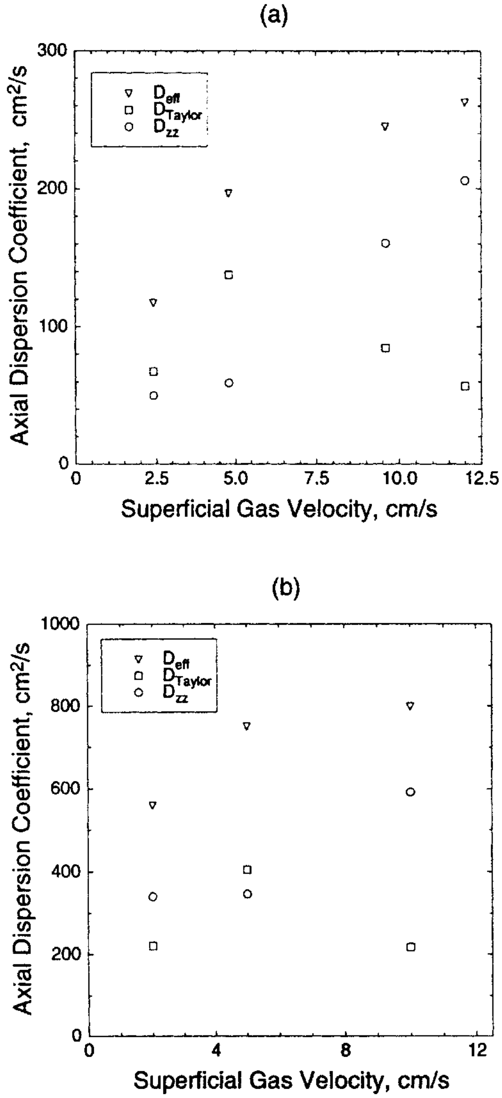

Figure 6. Effect of superficial gas velocity on the axial dispersion coefficient and its contributions, $\overline{D}_{zz}$ and D_{Taylor}, (from CARPT data): (a) D_c = 14 cm (6A); (b) D_c = 44 cm.

The effective axial dispersion coefficient, D_{eff}, has been calculated by the preceding procedure using CARPT data, for different operating conditions. Figure 7 displays the axial dispersion coefficient evaluated in the present work, with the experimentally measured axial dispersion coefficients from the literature, under similar (not same) operating conditions. The comparison between the two sets of results is encouraging, and validates the present method of evaluation of the axial dispersion coefficient using CARPT results for the fluid dynamic parameters.

Summary and Conclusions

Our analysis shows that the main contributing factors to liquid backmixing in bubble columns are liquid recirculation

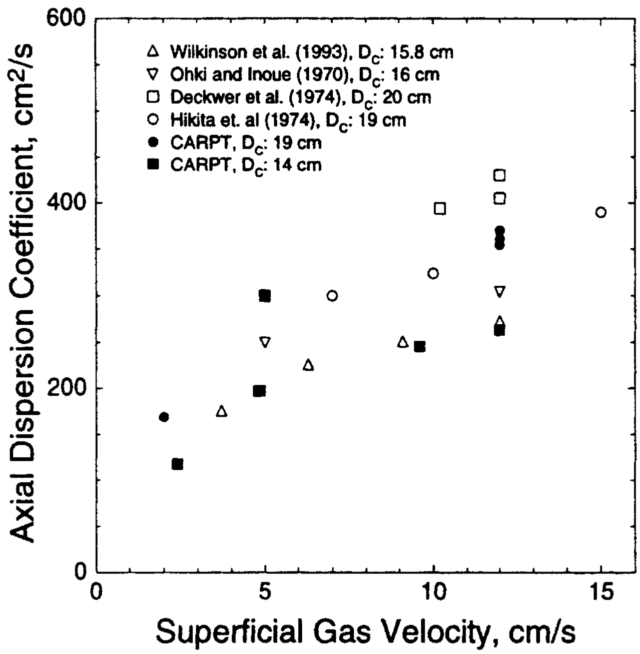

Figure 7. Axial dispersion coefficients: CARPT data vs. experimental data from the literature under similar operating conditions.

and eddy diffusion. The axial dispersion coefficient can be represented formally as a sum of two terms (Eq. 27), one that has the form of Taylor diffusivity (Eqs. 29 and 30) and encompasses the contributions of liquid recirculation velocity and radial eddy diffusivity as well as the liquid holdup profile, and the other (Eq. 28) that represents the cross-sectional mean axial eddy diffusivity. Clearly, these relationships are complex and this may partly explain why a universal correlation for the axial dispersion coefficient has not been found. The analysis presented in this article, however, allows us to examine the effect of changes in the fundamental fluid-dynamic parameters on the axial dispersion coefficient. Experimental measurements of the liquid holdup distribution using CT, and the liquid axial velocity and axial and radial eddy diffusivities, using CARPT, have been used to illustrate the trends in the axial dispersion coefficient.

Preliminary correlations for the relevant fluid-dynamic parameters that affect the axial dispersion coefficient have been proposed and are discussed elsewhere (Degaleesan et al., 1997). However, additional work at a variety of experimental conditions is needed for verification of their full range of application. By using these correlations, once they are verified, one can obtain a better understanding of the effects of operating conditions, such as high pressure and temperature, on the axial dispersion coefficient by examining their effect on the fluid-dynamic parameters that contribute to liquid backmixing. Such a study is part of the ongoing effort. Finally, it should be noted that the present analysis is only applicable to bubble columns of large L/D aspect ratio, where the flow is fully developed and one-dimensional in the middle section of the column. It is precisely for such conditions and in such geometries that the axial dispersion model is usually used to describe liquid backmixing in bubble columns.

Acknowledgments

We thank the Department of Energy (Contract DE-FC 22 95 PC950151) and the industrial sponsors of the Chemical Reaction Engineering Laboratory (CREL) for making this research possible. We appreciate the stimulating discussions with Dr. B. A. Toseland of Air Products and Chemicals, Inc.

Notation

g = acceleration due to gravity, cm/s^2
r = radial position, cm
R = column radius, cm
u_∞ = bubble rise velocity, cm/s
U_g = gas superficial velocity, cm/s
U_l = liquid superficial velocity, cm/s
z = axial position, cm
ϵ_g = gas holdup

Literature Cited

Anderson, K. G., "Analytical Prediction of Circulation and Dispersion in Bubble Columns," MS Thesis, Louisiana State Univ., Baton Rouge, LA (1989).

Argo, W. B., and D. R. Cova, "Longitudinal Mixing in Gas-Sparged Tubular Vessels," *Ind. Eng. Chem. Proc. Des. Dev.*, **4**, 352 (1965).

Baird, M. H., and R. G. Rice, "Axial Dispersion in Large Unbaffled Columns," *Chem. Eng. J.*, **9**, 171 (1975).

Berg, S., S. Schluter, and P.-M. Weinspach, "Ruckvermischung in Blasensaulen mit Einbauten," *Chem. Ing. Tech.*, **67**, 289 (1995).

Chen, J., P. Gupta, S. Degaleesan, F. Li, S. Roy, M. H. Al-Dahhan, and M. P. Duduković, "Column Scale Effects on Gas Holdup and Flow Pattern in Bubble Columns," AIChE Meeting, Los Angeles (1997).

Chen, R. C., J. Reese, and L.-S. Fan, "Flow Structure in a Three-Dimensional Bubble Column and a Three-Phase Fluidized Bed," *AIChE J.*, **40**, 1093 (1994).

Degaleesan, S., "Fluid Dynamic Measurements and Modeling of Liquid Mixing in Bubble Columns," DSc Thesis, Washington Univ., Saint Louis, MO (1997).

Degaleesan, S., M. P. Duduković, B. A. Toseland, and B. L. Bhatt, "A Two-Compartment Convective-Diffusion Model for Slurry Bubble Column Reactors," *Ind. Eng. Chem. Res.*, **36**, 4670 (1997).

Devanathan, N., D. Moslemian, and M. P. Duduković, "Flow Mapping in Bubble Columns Using CARPT," *Chem. Eng. Sci.*, **45**, 2285 (1990).

Devanathan, N., "Investigation of Liquid Hydrodynamics in Bubble Columns via Computer Automated Radioactive Particle Tracking (CARPT)," DSc Thesis, Washington Univ., Saint Louis, MO (1991).

Duduković, M. P., S. Degaleesan, P. Gupta, and S. B. Kumar, "Fluid Dynamics in Churn-Turbulent Bubble Columns: Measurements and Modeling," *Proc. ASME Fluids Eng. Div. Meeting*, Vancouver, BC (1997).

Fan, L.-S., *Gas-Liquid-Solid Fluidization Engineering*, Butterworths, Boston (1989).

Fan, L.-S., and K. Tsuchiya, *Bubble Wake Dynamics in Liquids and Liquid-Solid Suspensions*, Butterworth-Heinemann, Boston (1990).

Groen, J. S., R. F. Mudde, and H. E. A. van den Akker, "Time Dependent Behavior of the Flow in a Bubble Column," *Trans. Inst. Chem. Eng.*, A9 (1995).

Joshi, J. B., and M. M. Sharma, "A Circulation Cell Model for Bubble Columns," *Trans. Inst. Chem. Eng.*, **57**, 244 (1979).

Kumar, S. B., "Computed Tomography Measurements of Void Fraction and Modeling of the Flow in Bubble Columns," PhD Thesis, Florida Atlantic Univ., Boca Raton (1994).

Kumar, S. B., N. Devanathan, D. Moslemian, and M. P. Duduković, "Effect of Scale on Liquid Recirculation in Bubble Columns," *Chem. Eng. Sci.*, **49**, 5637 (1994).

Levenspiel, O., and T. J. Fitzgerald, "A Warning on the Misuse of the Dispersion Model," *Chem. Eng. Sci.*, **38**, 489 (1983).

Mashelkar, R. A., and P. A. Ramachandran, "Longitudinal Dispersion in Circulation Dominated Bubble Columns," *Trans. Inst. Chem. Eng.*, **53**, 274 (1975).
Miyauchi, T., S. Furusaki, S. Morooka, and Y. Akida, "Transport Phenomena and Reaction in Fluidized Catalyst Beds," *Advances in Chemical Engineering*, Vol. 11, T. B. Drew, G. R. Cokelet, J. W. Hoopes, Jr., and T. Vermeulen, eds., Academic Press, New York, p. 275 (1981).
Myers, K. J., "Liquid-Phase Mixing in Churn-Turbulent Bubble Columns," DSc Thesis, Washington Univ., St. Louis, MO (1986).
Myers, K. J., M. P. Duduković, and P. A. Ramachandran, "Modeling Churn Turbulent Bubble Columns: Liquid Phase Mixing," *Chem. Eng. Sci.*, **42**, 2301 (1987).
Ohki, Y., and H. Inoue, "Longitudinal Mixing of the Liquid Phase in Bubble Columns," *Chem. Eng. Sci.*, **25**, 1 (1970).
Riquarts, H.-P., "A Physical Model for Axial Mixing of the Liquid Phase for Heterogeneous Flow Regime in Bubble Columns," *Ger. Chem. Eng.*, **4**, 18 (1981).
Taylor, G. I., "The Dispersion of Matter in Turbulent Flow through a Pipe," *Proc. Roy. Soc. London*, **A223**, 446 (1954).
Ueyema, K., and T. Miyauchi, "Properties of Recirculating Turbulent Two Phase Flow in Gas Bubble Columns," *AIChE J.*, **25**, 258 (1979).
Wen, C. Y., and L. T. Fan, *Models for Flow Systems and Chemical Reactors*, Dekker, New York (1975).
Wilkinson, P. M., H. Haringa, F. P. A. Stokman, and L. L. van Dierendonck, "Liquid Mixing in a Bubble Column Under Pressure," *AIChE J.*, **48**, 1785 (1993).
Yang, Y. B., N. Devanathan, and M. P. Duduković, "Liquid Backmixing in Bubble Columns," *Chem. Eng. Sci.*, **47**, 2859 (1992).

Manuscript received Mar. 26, 1998, and revision received Aug. 27, 1998.